EU Horizon program: Horizon-CL4-2021-TWIN Transition

Reducing environmental footprint, improving circularity in extractive and processing value chains (IA)

Refractory Sorting Using Revolutionizing Classification Equipment

Grant Agreement No 101058310

WP 4 Preparation for sorting

D4.2 Testing of classification and sorting methods at laboratory scale

ReSoURCE

Project Reference No	101058310
Deliverable	4.2 Testing of classification and sorting methods at laboratory scale
Work Package	WP4
Type	R
Dissemination Level	PU
Date	November 2024
Status	Final
Editor(s)	Karl Friedrich, Christina Pölzl, Simone Neuhold, Stefan Heid, Alexander Leitner, Helmut Flachberger, Chandana Ratnayake
Contributor(s)	MUL, RHIM, SINTEF
Reviewers	All partners
Document description	Based on the content of report D 4.1, laboratory testing of classification and sorting methods will be conducted within task T 4.2. This will yield results which are delivered as report D 4.2.

Document revision history

Version	Date	Modification introduced	
		Modification reason	Author
V1.0	18.11.2024	First version	Karl Friedrich, Christina Pölzl, Simone Neuhold, Stefan Heid, Alexander Leitner, Helmut Flachberger, Chandana Ratnayake
V2.0	29.11.2024	Final version	Karl Friedrich, Christina Pölzl, Simone Neuhold, Stefan Heid, Alexander Leitner, Helmut Flachberger, Chandana Ratnayake

Executive Summary

The document examines advancements in recycling refractory materials, focusing on liberation evaluation methods and the scalability of comminution techniques. Efficient liberation and separation are critical for resource recovery, given the complex composition of refractories. The work reported in this deliverable refers to ReSoURCE project (*Resource - Refractory Sorting Using Revolutionizing Classification Equipment*) in the framework of WP4 – Preparation for sorting.

Two complementary methods were compared: 2D cross-section analysis and 3D density trials with ICP-MS analysis. The 2D method provides detailed insights into mineral phases, while the 3D approach captures bulk material behavior.

Conventional comminution methods, such as jaw, cone, and impact crushers, proved highly scalable and directly applicable to industrial operations. Semi-industrial trials validated their efficiency, eliminating the need for further upscaling.

In contrast, electrodynamic fragmentation (EDF) showed limitations for refractory recycling. Lab-scale trials indicated insufficient liberation for tightly bound materials and challenges integrating EDF's wet process into dry workflows.

The study highlights the importance of matching methods to material properties, with conventional techniques preferred for most scenarios. Combining proven approaches with innovative technologies offers potential for advancing refractory recycling and achieving sustainable solutions.

Table of Contents

1. Introduction

The sorting of refractory materials poses significant challenges in industrial settings due to the complex and heterogeneous nature of these materials. Refractories often consist of diverse mineral compositions, which complicate their effective separation and recycling. Efficient sorting is critical for optimizing the reuse of valuable components, reducing waste, and enhancing the sustainability of industrial processes. Addressing this challenge requires a systematic approach that begins with understanding and leveraging the intrinsic differences in material properties, such as composition, size, and shape, to ensure that sorting technologies, such as sensor-based systems, can effectively distinguish between material types. Effective sorting requires adequate particle liberation to enable the separation of valuable materials from waste fractions. Verifying liberation and sorting efficiency typically involves techniques such as microscopy, to analyze material structure, and density trials, to quantify the separation potential.

Proper preparation of feed material is crucial for sorting, with comminution processes playing a key role. Conventional size-reduction methods, such as crushing and grinding, are standard for achieving the required particle size. Alternate comminution techniques, such as electrodynamic fragmentation, have been explored for selective material liberation based on structural weaknesses. Transitioning these methods from laboratory or pilot-scale implementations to industrial-scale operations introduces challenges in scalability, throughput, and cost efficiency, which must be systematically addressed to meet industrial demands.

The goal of this approach is to create a seamless workflow that links the identification of usable property differences in refractory materials to the implementation of comminution techniques and their subsequent integration in sensor-based sorting. By systematically addressing each step, from particle liberation to industrial scalability, the goal is to develop an integrated, efficient, and sustainable sorting process tailored to the specific requirements of spent refractory material recycling.

1.1 Objectives

The sorting of refractory materials is a critical process in recycling and resource recovery, demanding careful consideration of property differences that enable efficient separation. Refractories, composed of different mineralogical and chemical phases, require methods that exploit their inherent distinctions, such as composition, density, size, and shape.

1. Evaluating Liberation Techniques: Compare 2D liberation evaluation using microscopy with 3D liberation evaluation using density trials and ICP-MS analysis. These methods aim to quantify the degree of material liberation and assess their suitability for improving sorting efficiency.

2. Upscaling Comminution Technologies: Assess the scalability of both conventional and alternative comminution processes. Evaluate semi-industrial pilot trials for their ability to replicate laboratory findings and meet the requirements of industrial-scale operations.

3. Integration into Sorting Processes: Link material property analysis, comminution, and sensor-based sorting technologies to create an efficient and sustainable workflow for recycling spent refractory materials.

2. Degree of Liberation - Fractional Class Analysis

Liberation is essential for separating spent refractory materials into their original components, making it a key step in recycling and resource recovery. For effective sorting, particles must be liberated to a degree where their distinct physical or chemical properties can be accurately detected and differentiated by sensors. Insufficient liberation results in agglomerates of mixed materials, reducing recovery rates and efficiency. Achieving proper liberation depends on comminution methods that break materials into distinct particles.

Comminution techniques, including conventional methods such as jaw crusher, impact crusher and cone crusher, as well as alternative approaches such as electrodynamic fragmentation, directly influence the liberation degree. Conventional methods typically apply mechanical forces to break materials down into smaller sizes, aiming to liberate the original components. While effective for some materials, this approach may not selectively target the interfaces between different phases, leading to incomplete liberation. Alternative methods, on the other hand, such as electrodynamic fragmentation, utilize high-energy pulses to exploit the structural weaknesses within materials. This technique supports selective breaking along grain boundaries and interfaces, targeting higher degrees of liberation while preserving particle integrity.

The degree of liberation has a direct impact on sorting efficiency in sensor-based systems. Sensors, such as laser-induced breakdown spectroscopy or optical scanners, rely on the exposure of individual material properties to detect and classify particles. Poorly liberated particles—where multiple material phases remain bonded—can produce inaccurate signals, complicating the sorting process and leading to contamination of the separated fractions. In contrast, well-liberated particles present clear and distinct signals, enabling sensors to achieve high accuracy and efficiency.

Moreover, liberation influences the scalability and economic viability of sorting processes. A high degree of particle liberation ensures consistent sorting performance, reducing inefficiencies and the need for reprocessing. Consequently, achieving optimal liberation during comminution not only enhances sorting efficiency but also lowers operational costs and energy consumption.

2.1 Materials

Refractory products find applications in high-temperature industrial processes, including steel, cement and glass production. The refractory lining is designed to protect critical process units such as furnaces and hot metal ladles against chemical, mechanical and thermal stress and is tailored for specific applications. After end-of-life, the lining is dismantled at the e.g., steel or cement production site, whereby a mixing of products and the generation of fine particles are unavoidable. Furthermore, the dismantling process leads to an unpredictable particle size distribution and adhesions (e.g., slag or clinker) can often not be fully removed.

In the ReSoURCE project, the focus is on spent refractories from steel casting ladles (SCL) and cement rotary kilns (CRK) with the main brick types: magnesia-based carbon bonded bricks and alumina-based carbon bonded bricks for SCL and magnesia spinel burned bricks (iron rich or iron poor) for CRK (see D1.1). For the D4.1 subchapter "Coarse comminution, < 120 mm" (described in chapter 1) RHIM provided pre-sorted and pre-processed (< 80 mm) breakout material from the cement and the steel industry. In total 3000 kg of the sorting classes "hercynite" (iron rich magnesia spinel bricks) and "MgO-C" (magnesia-based carbon bonded bricks) were sampled and crushed after manual sorting at RHIM MIRECO site in Mitterdorf, Austria. In addition, 50 kg of main raw materials used in magnesia carbon and magnesia spinel bricks were provided.

For the D4.1 subchapter "Conventional and alternate comminution, < 5 mm" approximately 30 kg of the same sorting classes, i.e., "MgO-C" and "hercynite" but from different feedstocks compared to the samples provided for "Coarse comminution, < 120 mm" were sampled and crushed (< 40 mm) at MIRECO site in Mitterdorf, Austria.

D4.2 focuses on the materials being produced by the different comminution processes, which were processed during the work for D4.1 "Conventional and alternate comminution, < 5 mm" utilizing different comminution aggregates: jaw crusher, impact crusher, cone crusher and electrodynamic fragmentation on lab-scale.

2.2 Methodology

D4.2 evaluates the difference between 2D liberation evaluation in cross-section analysis with microscopy and 3D liberation evaluation using density trials with ICP-MS analysis.

The primary distinction between those two methods lies in their dimensional approach: 2D liberation analysis provides detailed, high-resolution images of a sample's cross-section, while 3D liberation analysis offers a holistic view of material behavior across the entire sample volume. Both methods offer complementary advantages but also have inherent limitations.

2D liberation evaluation with microscopy and ImageJ Fiji is ideal for rapidly assessing phase distribution and liberation at high spatial resolution. It identifies phase boundaries, intergrowths, and surface features, making it ideal for preliminary investigations or visually analyzable materials. However, its reliance on cross-sectional images means it may miss important three-dimensional information.

On the other hand, 3D liberation analysis using density trials and ICP-MS analysis is more comprehensive, providing a complete volumetric perspective on material characteristics. This method effectively quantifies elemental composition and evaluates liberation efficiency, detecting enclosed phases invisible to microscopy.

2.3 2D Liberation Evaluation: Cross-section Analysis with Microscopy

2D liberation evaluation is a powerful technique for characterizing materials in industries like mining, metallurgy, and recycling, where understanding the degree of liberation is critical for optimizing separation processes. Liberation, in this context, refers to the extent to which valuable phases (e.g., minerals or metals) are physically separated from non-valuable phases (e.g., gangue or matrix).

Microscopy for 2D Liberation Analysis

Microscopy plays a central role in 2D liberation evaluation, with transmitted and reflected light microscopy offering complementary perspectives. Transmitted light microscopy is particularly suited for analyzing thin sections of materials, where light passes through the sample to reveal internal structures, including grain boundaries and inclusions. This technique is ideal for transparent or semi-transparent phases, such as quartz or other silicates, and provides critical insights into phase distribution and associations.

Reflected light microscopy, on the other hand, is used for opaque materials, such as metals and sulfides, where light reflects off the surface rather than passing through the sample. This method highlights surface features and phase boundaries in polished cross-sections, making it highly effective for analyzing metallic ores or recycling residues. Together, transmitted and reflected light microscopy enable a comprehensive evaluation of the material's internal composition and structure.

Analysis with ImageJ Fiji

The analysis of microscopy images obtained from transmitted and reflected light is enhanced using ImageJ Fiji, an open-source image analysis software. ImageJ Fiji offers a suite of tools for processing and quantifying images, making it possible to assess liberation quantitatively.

The procedure begins with image preprocessing (adjusting brightness, contrast, and noise reduction) to enhance clarity and highlight phase boundaries. Segmentation separates phases based on grayscale or color intensity (e.g., brighter regions for metals, darker for gangue). Using ImageJ Fiji, key parameters such as particle size, shape, and phase area fractions are measured to calculate the liberation degree, expressed as the percentage of the valuable phase exposed.

Combining microscopy with ImageJ Fiji provides high-resolution imaging, quantitative analysis, and dual validation for robust results.

The 2D nature of this analysis has limitations, as a single cross-section may not represent the 3D structure. Phases appearing liberated in two dimensions might remain connected in other dimensions, possibly leading to inaccurate evaluations. This can be addressed with multiple cross-sections or complementary 3D density trials.

2.4 3D Liberation Evaluation: Density Trials with ICP-MS analysis

3D liberation analysis characterizes materials by evaluating the separation of valuable components from reject materials. By integrating density trials and elemental analysis, this approach provides a comprehensive understanding of material behavior during comminution and separation processes, facilitating the optimization of resource recovery strategies.

Accurate elemental analysis is fundamental to material characterization and quality assessment. In this document, data from a handheld X-ray fluorescence (XRF) analyzer (e.g., Vanta) will be validated against measurements on the same samples using inductively coupled plasma mass spectrometry (ICP-MS). These techniques differ in measurement principles, precision, and sensitivity, which can lead to variations in results. Understanding these differences is key to accurate interpretation.

Measurement Principles

Handheld XRF analyzers operate on the principle of X-ray fluorescence. An X-ray source excites the atoms in a sample, causing the emission of secondary (fluorescent) X-rays characteristic of the elements present. These emissions are detected and analyzed to quantify the elemental composition. XRF is a non-destructive technique that excels at analyzing solid materials quickly and conveniently, often without requiring extensive sample preparation. However, it primarily detects elements with atomic numbers above 11 (sodium) and struggles with low concentrations (parts per million or less) due to limitations in detection sensitivity. (Beckhoff et al., 2006)

In contrast, ICP-MS utilizes inductively coupled plasma to ionize the elements in a sample. The sample is typically digested into a liquid form and introduced into the plasma, where high temperatures (around 10,000 K) ionize the atoms. These ions are then separated and quantified based on their mass-to-charge ratios using a mass spectrometer. ICP-MS offers exceptional sensitivity, capable of detecting trace elements at parts-per-billion (ppb) levels or lower, and can analyze a wide range of elements, including those that are challenging for XRF, such as lithium or boron. (Thomas, 2013)

Deviations in Measurement Results

The differences in measurement principles contribute to deviations in results when comparing XRF and ICP-MS analyses. XRF is influenced by matrix effects, surface roughness, and sample homogeneity. For instance, when analyzing heterogeneous materials such as ores or composite samples, XRF may yield less accurate results due to uneven element distribution or surface inconsistencies. In contrast, ICP-MS, which analyzes the sample in a homogenized liquid form, is less prone to such variability and provides more reliable results for inhomogeneous samples.

Elemental overlap and interference are another source of deviation. XRF can misidentify elements when their characteristic X-ray peaks overlap, particularly for neighboring elements on the periodic table. ICP-MS, though not immune to interference (e.g., isobaric overlaps or polyatomic ions), offers correction methods like collision or reaction cell technology to mitigate these effects, often resulting in more accurate results for complex samples.

Evaluation of the density trial fractions from D4.1 with ICP-MS analysis

The deviations between XRF and ICP-MS measurements should be interpreted in the context of their respective advantages and limitations. XRF is ideal for rapid, in-field analysis where non-destructive testing is paramount, such as in mining operations or quality control of materials. However, for applications requiring high sensitivity and precise quantification of trace elements, ICP-MS is the preferred choice due to its superior detection capabilities and resistance to surface or matrix-related artifacts.

For D4.2, it was decided to complement the handheld XRF measurements with ICP-MS analysis in D4.2. This approach aims to provide more detailed results, enabling a more precise interpretation of the 3D liberation evaluation.

2.5 Results

Fractional class analysis results are presented in two separate parts, the 2D liberation evaluation (cross-section analysis with microscopy) and the 3D liberation evaluation (density trials with ICP-MS analysis).

2D Liberation Evaluation: Cross-section Analysis with Microscopy

Using ImageJ Fiji, a color analysis of the reflected light images was conducted using the colors red, gray, white, and black. The pixels of each color were counted to determine the number and proportion of each color in every reflected light image. Each reflected light image, used to visualize the different grains in the cross-sections, is paired with the corresponding reflected light image.

The definitions and evaluation approach for each color are detailed below:

- **Pixel Color: Red**
    - Particles of the same type were identified and displayed uniformly in red.
    - The number of red pixels and their proportion were calculated to quantify those.
- **Pixel Color: Matrix (Gray)**
    - The matrix material was identified and displayed in gray.
    - The number and proportion of gray pixels were calculated to represent the matrix phase.
- **Pixel Color: Rest (White and Black)**
    - Pixels not categorized as red or gray were classified as "rest" and displayed in white or black.
    - The proportion of the rest was determined using the formula:

$$\text{Amount of Rest} = 100\ \% - \text{Amount of Red} - \text{Amount of Matrix}.$$

- **Total Number and Proportion of Pixels**
    - The total number of pixels in each sample image was calculated to ensure the proportions of red, gray, and rest add up to 100%.
    - The total proportion ("amount") is always 100%.

<u>Comparison of liberation results across different comminution aggregates</u>

The liberation degree of MgO-C and Hercynite A materials (particle size range 3.15–4 mm) was assessed following the trials described in D4.1, utilizing four comminution aggregates: jaw crusher, cone crusher, impact crusher, and EDF. While the analysis faced challenges due to the limited availability of microscopy images, the data provided valuable insights into the liberation behavior of these materials (Figure 1-7). Although no significant differences in liberation efficiency were identified among the aggregates for MgO-C or Hercynite A samples, the findings highlight the importance of enhancing data availability and exploring complementary evaluation techniques to support further refinement of comminution processes.

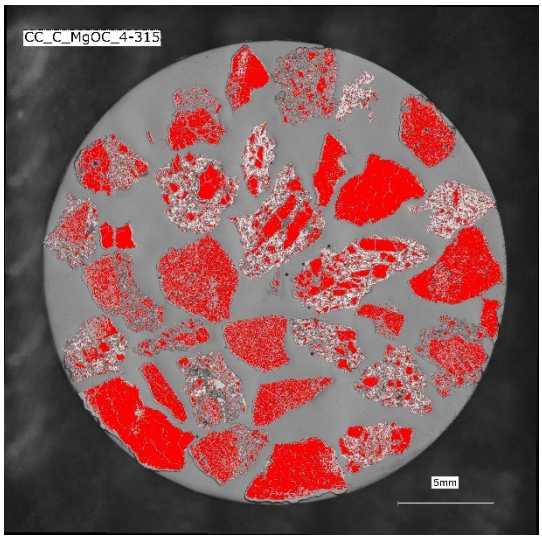

Figure 1: MgO-C sample - cone crusher

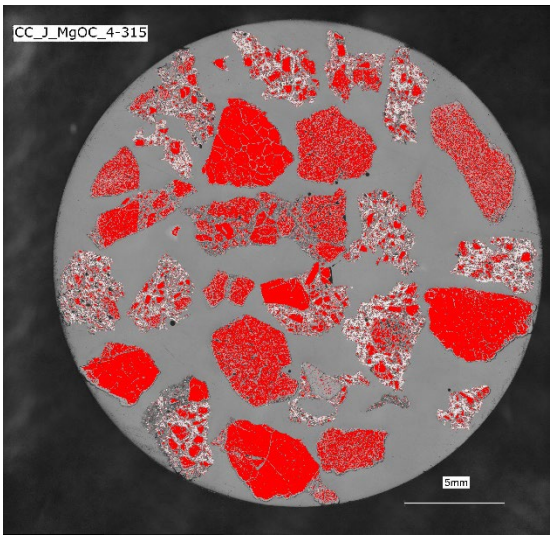

Figure 2: MgO-C sample - jaw crusher

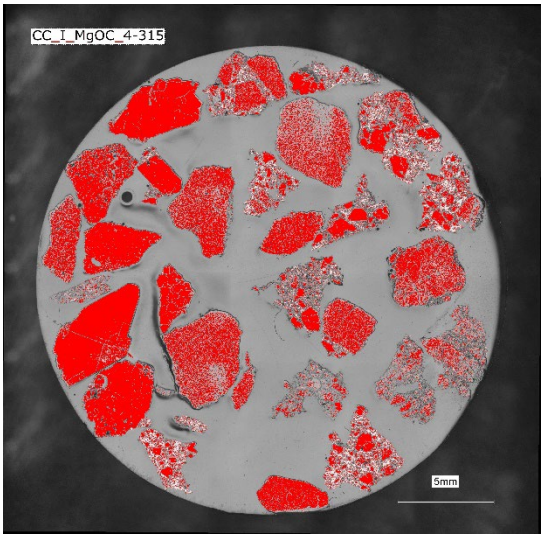

Figure 3: MgO-C sample - impact crusher

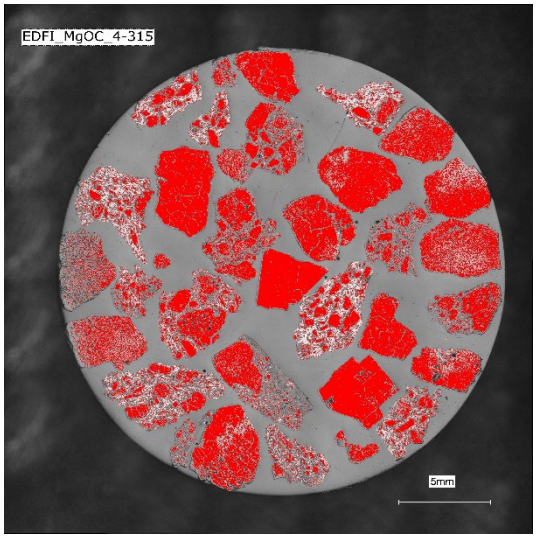

Figure 4: MgO-C sample - EDF

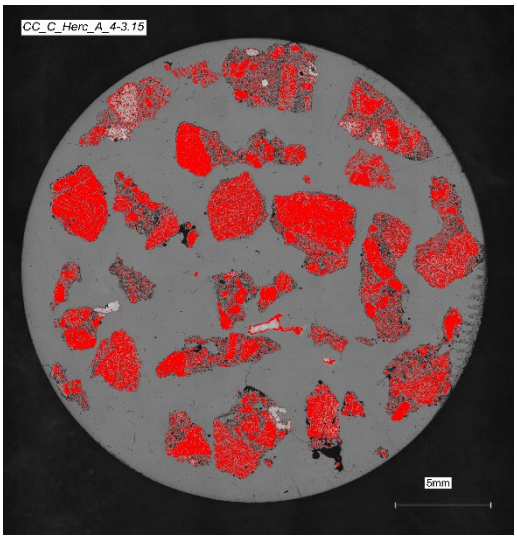

Figure 5: Hercynite A sample - cone crusher

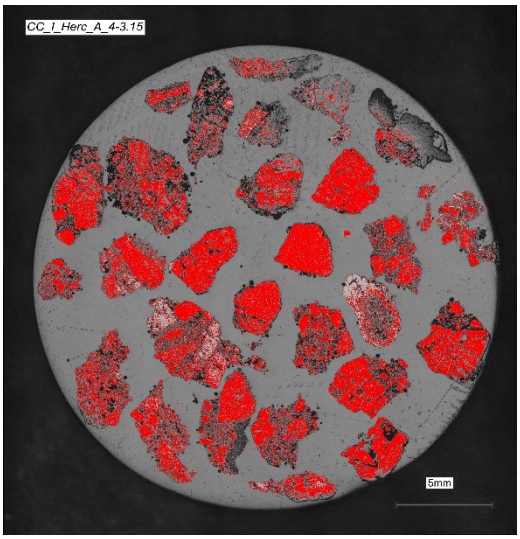

Figure 6: Hercynite A sample - jaw crusher

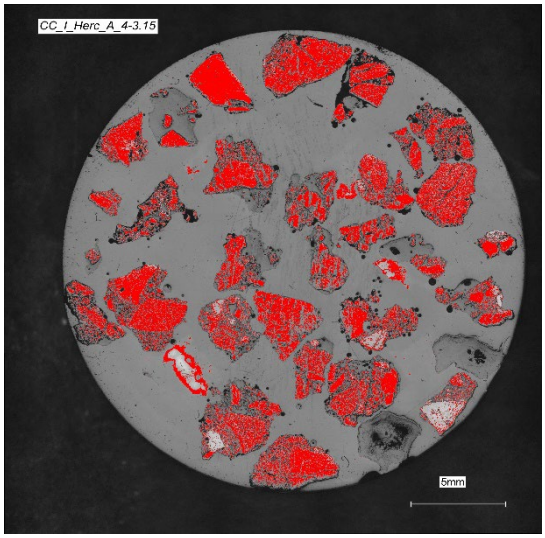

Figure 7: Hercynite A sample - impact crusher

The analysis of reflected light images using ImageJ Fiji improved phase identification and pixel quantification, representing progress toward more consistent evaluations and marking an initial step toward automated liberation analysis. However, further development is required to enable reliable calculation of the ratio between fully liberated and intergrown particles.

Example results from the 2D liberation evaluation are presented as follows:

- Figure 8 and Table 1: MgO-C sample analysis.
- Figure 9 and Table 2: Hercynite A sample analysis.
- Figure 10 and Table 3 : Hercynite B sample analysis.

All samples shown below were processed using a jaw crusher and analyzed within the particle size range of 3.15–4 mm.

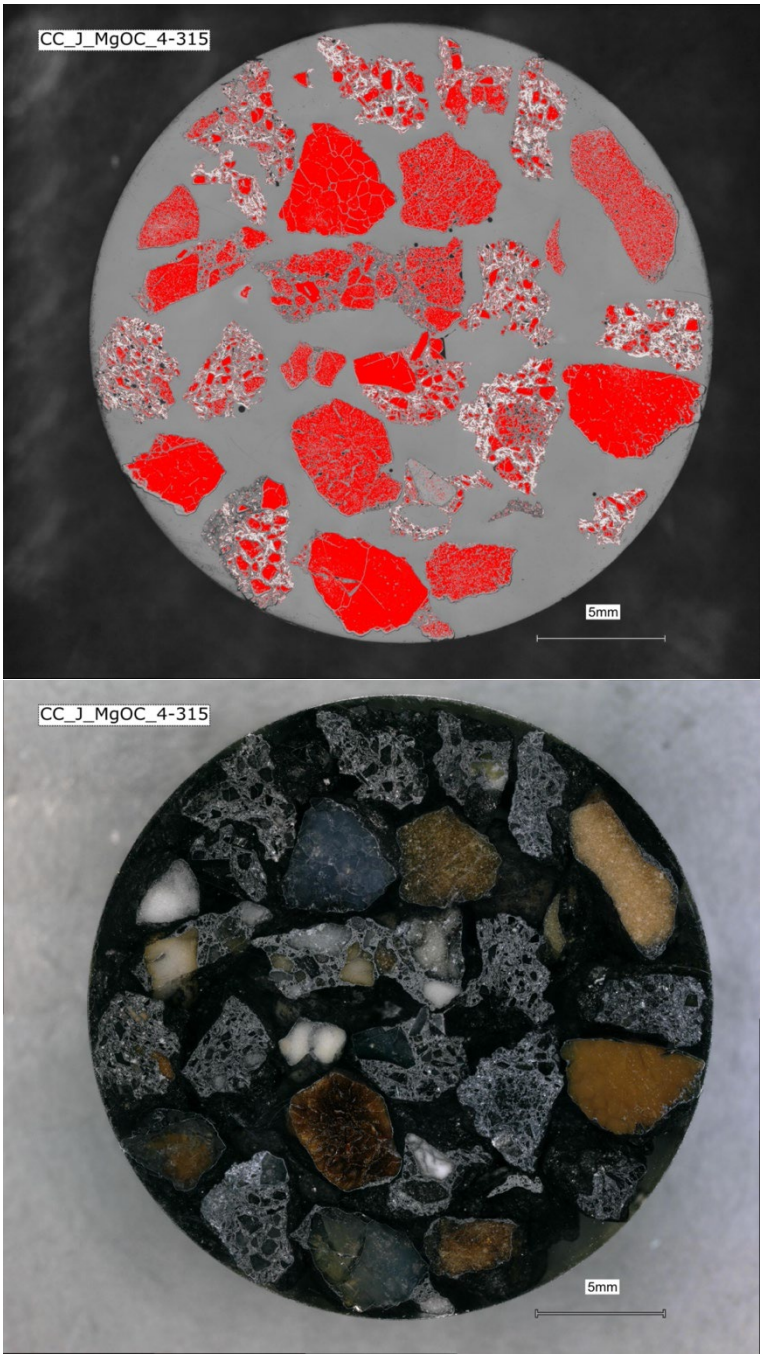

Figure 8: CC_J_MgOC_4-3.15, MgO-C comminution method: jaw crusher; particle size range: 4-3.15 mm, imageJ fiji evaluation for the reflected light microscopy image above, reflection light microscopy image below.

Table 1: CC_J_MgOC_4-3.15, MgO-C comminution method: jaw crusher; particle size range: 4-3.15 mm, imageJ fiji evaluation in numbers and amount of pixels.

Pixel colour	Number of pixels [-]	Amount [%]
Red	17,899	20.11
Matrix (gray)	107,534	62.23
Rest (white, black)	30,513	17.66
Sum	155,946	100.00

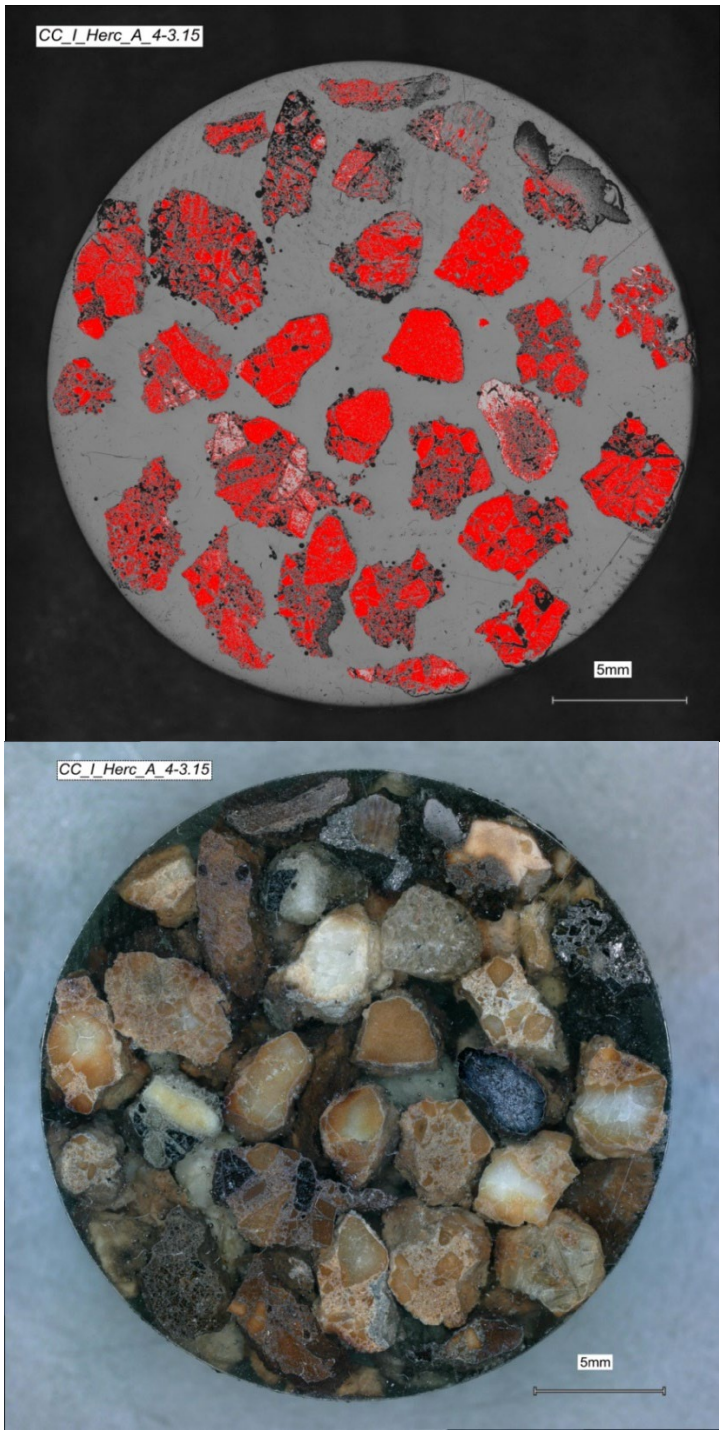

Figure 9: CC_J_Herc_A_4-3.15, Hercynite A comminution method: jaw crusher; particle size range: 4-3.15 mm, imageJ fiji evaluation for the reflected light microscopy image above, reflection light microscopy image below.

Table 2: CC_J_Herc_A_4-3.15, Hercynite A comminution method: jaw crusher; particle size range: 4-3.15 mm, imageJ fiji evaluation in numbers and amount of pixels.

Pixel colour	Number of pixels [-]	Amount [%]
Red	18,911	20.38
Matrix (gray)	98,534	45.75
Rest (white, black)	72,949	33.87
Summary	190,394	100.00

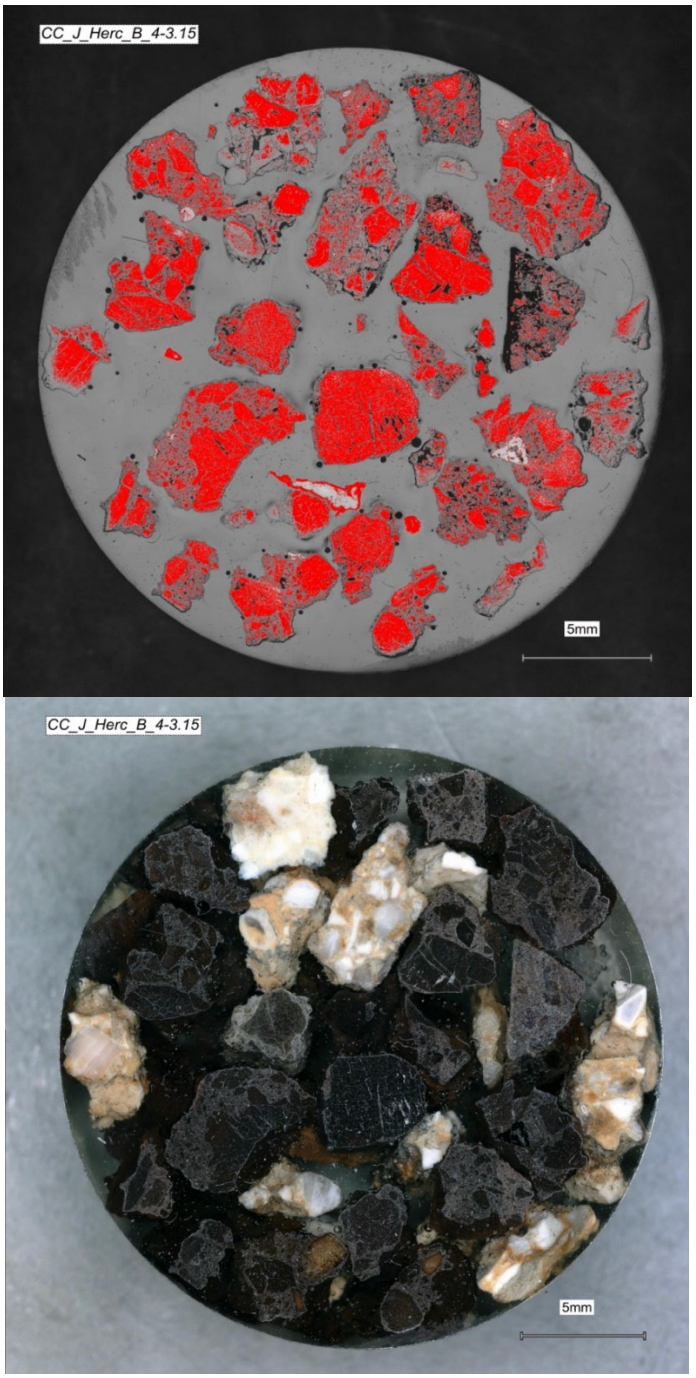

Figure 10: CC_J_Herc_B_4-3.15, Hercynite B comminution method: jaw crusher; particle size range: 4-3.15 mm, imageJ fiji evaluation for the reflected light microscopy image above, reflection light microscopy image below.

Table 3: CC_J_Herc_B_4-3.15, Hercynite B comminution method: jaw crusher; particle size range: 4-3.15 mm, imageJ fiji evaluation in numbers and amount of pixels.

Pixel colour	Number of pixels [-]	Amount [%]
Red	25,114	20.50
Matrix (gray)	89,891	45.39
Rest (white, black)	67,572	34.12
Summary	182,577	100.00

The results for all reflected light images evaluated with imageJ fiji can be seen in Table 4.

Interpreting the results requires combining the cross-section images with the image evaluation data presented in Table 4. Therefore, the interpretation must be performed individually for each sample. As examples, detailed explanations are provided for the three samples highlighted in dark gray.

- CC_J_MgOC_4-3.15

In Figure 8, four grains are almost completely red, indicating they are fully liberated with no matrix material. Thirteen grains, predominantly grey with a significant mix of red, are considered poorly liberated. Six grains with a higher proportion of red compared to grey are classified as sufficiently liberated.

- CC_J_Herc_A_4-3.15

Figure 9 shows four grains that are almost entirely red, classifying them as fully liberated, with no matrix material. Twenty-four grains exhibit a mix of grey and red, with grey dominating, categorizing them as poorly liberated. Additionally, two black grains are identified as impurities and are not relevant for liberation analysis.

- CC_J_Herc_B_4-3.15

In Figure 10, only one grain is nearly entirely red, identifying it as fully liberated. Twenty-two grains show a mix of red and grey pixels, with grey being dominant, classifying them as poorly liberated. A single black grain is observed, considered an impurity and irrelevant to the liberation evaluation.

Table 4: Results for all cross-section reflected light images evaluated with imageJ fiji.

Pixel colour	Red		Grey (matrix)		White / black (Rest)		Sum	
Sample	Number of pixels [-]	Amount [%]	Number of pixels [-]	Amount [%]	Number of pixels [-]	Amount [%]	Number of pixels [-]	Amount [%]
CC_C_Herc_A_4-3.15	19,491	19.00	119,882	54.64	57,842	26.36	197,215	100.00
CC_C_Herc_A_3.15-1	16,899	25.11	107,534	45.23	70,508	29.66	194,941	100.00
CC_C_Herc_B_4-3.15	21,355	28.83	106,200	44.40	64,024	26.77	191,579	100.00
CC_C_Herc_B_3.15-1	27,396	24.95	72,052	53.19	29,611	21.86	129,059	100.00
CC_C_MgOC_4-3.15	63,007	27.78	91,555	35.78	93,259	36.44	247,821	100.00
CC_C_MgOC_3.15-1	54,937	25.08	101,673	42.27	78,533	32.65	235,143	100.00
CC_I_Herc_A_4-3.15	56,724	25.70	95,940	39.10	86,387	35.20	239,051	100.00
CC_I_Herc_A_3.15-1	20,018	23.61	102,295	45.47	69,578	30.92	191,891	100.00
CC_I_Herc_B_4-3.15	18,911	20.38	98,534	45.75	70,950	33.87	188,395	100.00
CC_I_Herc_B_3.15-1	26,950	24.11	95,894	47.26	58,094	28.63	180,938	100.00
CC_I_MgOC_4-3.15	18,015	22.51	95,367	50.87	49,892	26.62	163,274	100.00
CC_I_MgOC_3.15-1	40,834	22.15	80,930	26.50	156,818	51.35	278,582	100.00
CC_J_Herc_A_4-3.15	18,911	20.38	98,534	45.75	72,949	33.87	190,394	100.00
CC_J_Herc_A_3.15-1	17,669	21.44	74,193	50.12	42,100	28.44	133,962	100.00
CC_J_Herc_B_4-3.15	25,114	20.50	89,891	45.39	67,572	34.12	182,577	100.00
CC_J_Herc_B_3.15-1	23,523	21.62	82,030	50.73	44,708	27.65	150,261	100.00
CC_J_MgOC_4-3.15	17,899	20.11	107,534	62.23	30,513	17.66	155,946	100.00
CC_J_MgOC_3.15-1	40,562	23.95	88,593	39.75	80,916	36.30	210,071	100.00
EDFL_MgOC_IV_5-10_4-3.15	39,101	25.23	114,577	35.69	125,457	39.08	279,135	100.00
EDFL_MgOC_IV_5-10_3.15-1	73,307	24.12	102,743	42.40	81,121	33.48	257,171	100.00

3D Liberation Evaluation: Density Trials with ICP-MS analysis

Building on the fractional class analysis performed in D4.1, an additional evaluation using the XRF handheld device (Vanta) will be conducted to validate the feasibility of the results.

To achieve this, ICP-MS analysis is performed to quantify magnesium (Mg) in MgO-C refractory samples and magnesium (Mg), iron (Fe), and aluminum (Al) in Hercynite A and B refractory samples. This approach also helps assess whether detailed ICP-MS analysis is necessary for refractory recycling or if the faster XRF handheld method provides sufficient accuracy for practical applications.

The results of the element analysis comparison method for MgO-C can be seen in Table 5.

Table 5: Comparison of XRF handheld and LECO to ICP-MS analysis for the comminuted MgO-C samples.

Refractory	Comminution technology	Particle size [mm]	m sample [g]	density [g/cm³]	m sample [g]	m (ICP-MS) [g]	Mg (XRF) [%]	Mg (ICP-MS) [%]	Mg (ICP-MS) [mg/kg]
MgO-C	Conventional, Jaw crusher	4-3.15	32.5	<3.0	6.8	0.3	32.3	27.7	276,813
				>3.0	25.4	0.3	58.5	26.2	262,192
		3.15-1	42.5	<3.0	11.5	0.3	32.7	17.1	170,633
				>3.0	30.5	0.3	40.8	20.4	204,226
		<1	5.0	-	5.0	-	44.7	-	-
	Conventional, Impact crusher	4-3.15	22.5	<3.0	6.4	0.3	40.7	24.1	241,441
				>3.0	16.0	0.3	49.9	23.5	235,341
		3.15-1	110.0	<3.0	27.4	0.3	30.4	23.3	233,237
				>3.0	82.4	0.3	37.0	28.9	288,856
		<1	5.0	-	5.0	0.3	43.2	17.5	175,410
	Conventional, Cone crusher	4-3.15	18.0	<3.0	4.2	0.3	41.2	21.2	212,484
				>3.0	13.5	0.3	51.0	26.1	260,792
		3.15-1	115.0	<3.0	86.2	0.3	44.1	23.6	235,619
				>3.0	27.3	0.3	34.8	23.5	234,933
		<1	5.0	-	5.0	0.3	46.8	16.0	160,271
	EDF Lab, 5-10 mm, sample IV	4-3.15	25.5	<3.0	9.3	0.3	39.3	24.8	248,227
				>3.0	15.7	0.3	45.5	37.4	374,224
		3.15-1	75.0	<3.0	30.0	0.3	30.0	20.5	204,794
				>3.0	44.4	0.3	21.5	30.6	306,216
		<1	5.0	-	5.0	0.3	38.5	16.4	164,419

m sample [g]	Mass of the sample, which was used for the density tests
m ICP-MS [g]	Mass of the sample, which was used for ICP-MS
Density [g/cm³]	Density class in which fraction enriched after the separation process
ICP-MS [%]	Element amount from ICP-MS
ICP-MS [mg/kg]	Element mass from ICP-MS
Marked in red	Values from ICP-MS lower than XRF

Values for the Mg content measured with ICP-MS that are lower than those measured with the XRF handheld are marked in red in the column “Mg (ICP-MS) [g]”. It is clearly visible that all measured values, except one, show that the ICP-MS results are lower than those obtained with the XRF handheld. The largest deviation is observed in the MgO-C sample comminuted with a jaw crusher, with a particle size range of 3.15-1 mm and a density higher than 3 g/cm³, where the XRF measured 58.6% Mg, and the ICP-MS measured 26.2% Mg. For the only fraction showing a lower Mg result for the XRF handheld than for the ICP-MS analysis, it should be noted that the MgO-C sample comminuted with EDF lab, with a particle size range of 3.15-1 mm and a density higher than 3 g/cm³, showed very low enrichment of Mg in its density class in D4.1. This indicates that the sample may have exhibited atypical behavior during the fractional class analysis, potentially influenced by variations or inconsistencies in sample preparation prior to the XRF measurement.

The discrepancy between Mg measurements using a handheld XRF device and ICP-MS for MgO-C samples, where XRF consistently yields higher values, can be attributed to several factors intrinsic to the methods and the characteristics of the material being analyzed. XRF measures the elemental composition of a sample by detecting secondary X-rays emitted when the sample is irradiated with primary X-rays. This technique is non-destructive and typically analyzes the surface or near-surface regions of the material. For MgO-C samples, which contain MgO and carbon, XRF may overestimate magnesium content due to its inability to differentiate effectively between the elemental form of Mg and its compound (MgO). The calibration of XRF for Mg often assumes homogeneity and does not account for matrix effects caused by high carbon content or irregular distribution of MgO in the sample. This can lead to interference and an overestimation of magnesium, especially if the XRF device interprets signal contributions from other compounds or contamination.

In contrast, ICP-MS involves the dissolution of the sample into a liquid phase, providing a bulk analysis of the material's composition. For MgO-C samples, the high carbon content might cause XRF signals to scatter or absorb differently than during ICP-MS analysis. Additionally, magnesium might be unevenly distributed in the sample, with surface regions richer in MgO compared to the bulk. Since XRF primarily evaluates the surface, it may give a distorted representation of the magnesium content.

Another contributing factor is the calibration standards used for both methods. XRF devices are often calibrated with standard reference materials that may not precisely match the complex composition of refractory material. If the calibration standards have a lower carbon content or different MgO distributions, the XRF device may misattribute part of the signal to magnesium, inflating the measured values. ICP-MS is less prone to such calibration errors since it analyzes dissolved elements in solution, providing a more representative assessment of the sample's overall composition.

For the comparison of the XRF handheld and the ICP-MS element analysis for hercynite the results can be seen in Table 6.

Table 6: Comparison of XRF handheld and LECO to ICP-MS analysis for the comminuted hercynite samples.

Refractory	Comminution technology	Particle size [mm]	m sample [g]	density [g/cm³]	m sample [g]	m ICP-MS [g]	Fe (XRF) [%]	Fe (ICP-MS) [%]	Fe (ICP-MS) [mg/kg]	Al (XRF) [%]	Al (ICP-MS) [%]	Al (ICP-MS) [mg/kg]	Mg (XRF) [%]	Mg (ICP-MS) [%]	Mg (ICP-MS) [mg/kg]
Hercynite high Fe (B)	Conventional, Jaw crusher	4–3.15	22.0	<3.63	21.5	0.3	0.6	3.2	31,590	2.8	2.6	26,488	30.5	32.5	324,696
				>3.63	0.3	-	8.6	-	-	7.0	-	-	16.2	-	-
		3.15–1	61.0	<3.63	51.2	0.3	0.4	2.8	28,067	0.6	3.7	36,638	38.0	28.3	282,926
				>3.63	9.3	0.3	0.6	10.0	100,148	0.9	3.4	33,999	51.3	26.4	263,907
		<1	5.0	-	5.0	-	2.9	-	-	9.7	-	-	18.1	-	-
	Conventional, Impact crusher	4–3.15	15.0	<3.63	14.3	0.3	1.6	2.7	26,891	8.8	3.1	31,144	29.8	28.0	280,301
				>3.63	0.4	-	0.7	-	-	4.5	-	-	30.6	-	-
		3.15–1	45.0	<3.63	40.5	0.3	1.5	2.5	24,885	15.2	3.9	39,104	18.8	25.8	257,780
				>3.63	4.0	0.3	13.8	11.9	118,583	12.9	6.0	59,843	17.3	32.1	321,003
		<1	5.0	-	5.0	-	3.3	-	-	8.5	-	-	16.3	-	-
	Conventional, Cone crusher	4–3.15	22.5	<3.63	22.1	0.3	1.2	3.0	30,223	3.4	3.3	32,676	46.7	30.4	304,275
				>3.63	0.2	-	0.5	-	-	9.8	-	-	19.3	-	-
		3.15–1	43.0	<3.63	37.2	0.3	1.1	3.0	30,252	4.8	3.9	39,010	45.7	25.6	256,322
				>3.63	5.0	0.3	1.2	7.3	72,685	4.5	4.9	48,699	45.0	28.4	283,795
		<1	5.0	-	5.0	-	2.8	-	-	9.4	-	-	14.5	-	-
Hercynite low Fe (A)	Conventional, Jaw crusher	4–3.15	22.5	<3.63	21.3	0.3	4.3	1.7	16,977	1.6	1.2	11,642	39.1	29.6	295,582
				>3.63	0.8	-	12.7	-	-	10.5	-	-	16.2	-	-
		3.15–1	42.0	<3.63	38.8	0.3	3.5	2.0	20,294	2.7	1.4	14,051	39.0	41.0	410,006
				>3.63	2.6	0.3	15.5	14.4	144,398	9.1	9.5	95,277	21.8	26.0	260,164
		<1	5.0	-	5.0	-	3.6	-	-	2.9	-	-	25.8	-	-
	Conventional, Impact crusher	4–3.15	15.0	<3.63	14.3	0.3	3.2	1.4	13,589	5.8	1.1	11,291	33.6	37.9	378,575
				>3.63	0.4	-	8.7	-	-	10.2	-	-	23.4	-	-
		3.15–1	45.0	<3.63	40.5	0.3	0.8	1.7	17,320	3.2	1.4	14,468	34.5	36.5	365,080
				>3.63	4.0	0.3	2.2	8.9	88,504	5.1	6.9	69,199	41.3	27.0	269,725
		<1	5.0	-	5.0	-	3.4	-	-	2.9	-	-	28.9	-	-
	Conventional, Cone crusher	4–3.15	20.0	<3.63	19.5	0.3	2.0	1.7	17,385	3.2	1.3	12,731	49.5	35.6	355,649
				>3.63	0.2	0.3	15.0	1.6	15,592	15.1	1.5	14,637	16.2	32.6	326,013
		3.15–1	48.5	<3.63	43.4	0.3	2.5	1.7	16,508	3.6	1.4	14,057	32.2	37.0	369,996
				>3.63	4.5	0.3	1.8	9.5	95,078	4.0	3.6	36,410	36.6	29.7	296,716
		<1	5.0	-	5.0	-	3.0	-	-	2.8	-	-	26.2	-	-

m sample [g]	Mass of the sample, which was used for the density tests
m ICP-MS [g]	Mass of the sample, which was used for ICP-MS
Density [g/cm³]	Density class in which fraction enriched after the separation process
ICP-MS [%]	Element amount from ICP-MS
ICP-MS [mg/kg]	Element mass from ICP-MS
Marked in red	Values from ICP-MS lower than XRF

Values for Mg, Fe, or Al content measured with ICP-MS that are lower than those measured with the XRF handheld are marked in red in the column “Element (ICP-MS) [g]”. There is no clear trend for any of the elements, as ICP-MS sometimes shows higher results and sometimes lower results compared to the XRF handheld. Therefore, a comparison of the measurement methods for hercynite is not feasible with the measured element values. For hercynite, the appropriate measurement method must be chosen for each element separately by comparing the methods to the corresponding expected element content from refractory manufacturing.

Additionally, it should be noted that for some samples, either no sample was available, or the mass was too low to measure with ICP-MS. These are indicated by “-“ in Table 6 for density-separated samples.

For Mg, XRF results may be inflated because magnesium emits low-energy X-rays that are more prone to attenuation or scattering within the sample or the surrounding matrix. Matrix effects in hercynite, particularly its high density and potential inclusions of other phases, can interfere with Mg signal detection. In contrast, ICP-MS overcomes this issue by fully digesting the sample and analyzing dissolved ions, providing a more precise Mg concentration.

For Fe, which is present in concentrations below 15%, XRF may underestimate its levels due to the calibration of the device. If the calibration standards used in the XRF device have significantly different

Fe contents or matrices, the results may not adequately reflect hercynite's composition. Additionally, Fe's fluorescence signal might be partially absorbed by surrounding minerals in the sample, leading to lower apparent values. ICP-MS, however, is less affected by such matrix effects and is likely to produce more accurate Fe measurements.

For Al, with concentrations below 6%, XRF is prone to overestimation or underestimation depending on the matrix effects and sample preparation. Alumina emits very low-energy X-rays, which can be attenuated by the surrounding material or even by surface roughness. Furthermore, XRF's calibration may not be ideal for detecting Al at low concentrations in a dense mineral like hercynite. ICP-MS, due to its high sensitivity for trace elements, provides a more reliable measurement of Al, especially at low concentrations.

When the Fe content is below 16% and Al is below 7%, ICP-MS is likely the more accurate method. Its dissolution-based analysis eliminates surface and matrix effects, ensuring a representative and precise measurement. While XRF is convenient for rapid, non-destructive surface analysis, its accuracy diminishes for light elements like Mg and Al and for elements present in low concentrations like Fe in hercynite. The limitations of XRF calibration, matrix interference, and surface bias make it less reliable for these measurements. Thus, for hercynite samples, ICP-MS is the preferred technique for precise and consistent elemental analysis.

3. Upscaling: Conventional and Alternate Comminution Methods

Comminution, the process of reducing the size of solid materials, is crucial for liberating the valuable phases from the surrounding matrix, which directly impacts the efficiency of sorting technologies. Upscaling these processes presents several technical and operational challenges that must be addressed to ensure successful large-scale implementation.

D4.2 provides the upscaling opportunities of the conventional and alternate comminution methods, which were evaluated in D4.1: jaw crusher, impact crusher, cone crusher and electrodynamic fragmentation.

3.1 Conventional Comminution

Comprehensive comminution experiments at RHI Magnesita GmbH and ARP GmbH have provided valuable insights into the performance and behavior of various crushing equipment for processing breakout materials from the cement and steel industries (Hercynite and MgO-C). The trials, focused on coarse comminution of pre-crushed material (< 120 mm), evaluated the efficiency of jaw, cone, and impact crushers in achieving target particle size distributions while minimizing fines production.

Those conventional semi-industrial-scale comminution trials conducted in D4.1 are directly applicable to industrial processes, eliminating the need for additional upscaling trials.

One of the primary reasons semi-industrial trials are directly applicable to industrial processes is the similarity in equipment design and operational principles. Semi-industrial trials typically use scaled-down versions of industrial machinery, such as crushers, ball mills, or high-pressure grinding rolls, which are designed to replicate the key mechanical, hydraulic, and energy-transfer mechanisms of their larger counterparts. By preserving these core features, the trials accurately simulate how materials behave under industrial conditions, including particle breakage patterns, energy consumption, and wear dynamics. Furthermore, these trials often operate at throughputs and energy inputs that align proportionally with industrial requirements, ensuring that the process is directly scalable.

3.2 Electrodynamic fragmentation

Electrodynamic fragmentation relies on the sudden release of electrical energy stored in capacitors. When discharged through electrodes submerged in a liquid medium (usually water), this energy generates plasma channels, resulting in shock waves and tensile forces. These forces propagate through the material, causing fractures along grain boundaries, phase interfaces, or other structural weak points. The process is particularly advantageous for delaminating composites, liberating precious metals from electronic waste, and separating minerals in mining applications.

At the laboratory scale, EDF systems typically operate with batch processing, where small amounts of material are treated in controlled conditions. To move toward semi-industrial scale, a shift to continuous processing and larger volumes is necessary.

Challenges in upscaling electrodynamic fragmentation processes

Since systems for electrodynamic fragmentation on lab-scale and semi-industrial scale differ from each other, there are a few challenges in upscaling this process.

1. Material throughput and process integration

Laboratory systems are typically batch-based, processing small quantities in short cycles. Scaling up requires continuous material handling systems to accommodate larger volumes and improve throughput. Integrating EDF with conveyor systems or rotary drums can enable semi-continuous processing. Careful control of material feed rates, water flow, and discharge timing is essential to maintain efficiency.

2. Water treatment and environmental considerations

Large-scale EDF systems generate wastewater containing fine particles and dissolved metals, requiring treatment before discharge or reuse. Incorporating closed-loop water recycling systems with filtration and chemical treatment can reduce water consumption and environmental impact. Monitoring systems for water quality and pollutant levels can ensure compliance with environmental regulations.

3. Scaling equipment size and safety

Upscaling EDF requires larger reaction chambers and higher-capacity systems, which introduce new safety concerns, such as managing high-voltage arcs and ensuring operator protection. Designing modular, compact reactor units with robust insulation and interlocking safety mechanisms can mitigate risks.

EDF upscaling to semi-industrial scale: MgO-C

Establishing pilot plants for semi-industrial EDF systems is crucial for validating scalability. Therefore, the selFrag Lab 2.1 trials from D4.1 are upscaled and transferred to the selFrag Pre-Weakening Test Station (PWTS) (Figure 11) in Kerzers, Switzerland, in D4.2.

The upscaling process from the selFrag Lab 2.1, a laboratory-scale electrodynamic fragmentation system, to the selFrag Pre-Weakening Test Station, a pilot-scale system, is designed to ensure that results are directly comparable by maintaining consistent process parameters and methodology while scaling up throughput. This transition involves careful adjustments to preserve the physical principles and mechanisms of electrodynamic fragmentation while accommodating the larger scale and operation. The key to ensuring comparability lies in replicating the electric pulse characteristics—such as voltage, pulse energy, frequency, and the dielectric medium's properties—between the two systems. By maintaining these parameters, the underlying fragmentation mechanism remains consistent, producing comparable liberation patterns.

To compare and upscale the process for MgO-C, the electrode distance was set to 40 mm and the frequency to 5 Hz. These are the maximum settings for the selFrag Lab 2.1 and the minimum settings for the selFrag PWTS.

The primary difference in upscaling lies in the design of the systems. The selFrag Lab 2.1 operates as a closed system with a process vessel, which introduces an electrohydraulic explosion effect during electrodynamic fragmentation. This effect could influence the liberation results, making them potentially different from those achieved with the selFrag PWTS, which features a continuous throughput and an open system design.

Figure 11: selFrag Pre-Weakening Test Station (PWTS) in Kerzers, Switzerland.

The PWTS was set up with voltage and pulses to match the “EDF lab, 5-10 mm, sample IV” by configuring the generator stages to 4 and the capacity to 150 nF. The comminution results and the potential for upscaling EDF for MgO-C comminution were evaluated using 3D liberation with density tests and element analysis.

Table 7 shows that upscaling from the selFrag Lab 2.1 to the selFrag Pre-Weakening Test Station is effective. The 3D liberation evaluation, through density tests and element analysis, shows consistent results across both systems. Comparing the green cells for EDF lab and EDF semi-industrial indicates that the electrodynamic fragmentation mechanisms work similarly at both scales. By replicating key process parameters and ensuring uniform sample preparation, the lab-scale results are directly translatable to the pilot-scale station. The comparable outcomes in liberation degree and material separation efficiency, confirmed by density trials and ICP-MS analyses, validate the scalability of the process. This consistency ensures that the larger-scale system reflects the lab-scale unit’s performance, enabling reliable industrial predictions without additional calibration or extensive adjustments.

Table 7: EDF upscaling result, MgO-C, 3D liberation evaluation with density tests and element analysis.

Refractory	Comminution technology	Particle size [mm]	m sample [g]	density [g/cm³]	m sample [g]	C (LECO) [%]	M (ICP-MS) [g]	Mg (XRF) [%]	Mg (ICP-MS) [%]	Mg (ICP-MS) [mg/kg]
MgO-C	EDF Lab, 5–10 mm, sample IV	4–3.15	25.5	<3.0	9.3	18.9	0.3	39.3	24.8	248,227
				>3.0	15.7	2.4	0.3	45.5	37.4	374,224
		3.15–1	75.0	<3.0	30.0	20.9	0.3	30.0	20.5	204,794
				>3.0	44.4	5.1	0.3	21.5	30.6	306,216
		<1	5.0	-	5.0	16.9	0.3	38.5	16.4	164,419
	EDF I, V1	4–3.15	22.5	<3.0	35,1	19,5	0,3	38,0	29,8	297634,2
				>3.0	56,8	2,4	0,3	48,2	15,3	153422,4
		3.15–1	110.0	<3.0	18,6	21,7	0,3	37,9	28,7	287126,2
				>3.0	30,7	2,8	0,3	54,0	20,1	200928,1
		<1	5.0	-	5,0	18,2	0,3	43,2	-	-

m sample [g]	Mass of the sample, which was used for the density tests
m ICP-MS [g]	Mass of the sample, which was used for ICP-MS
Density [g/cm³]	Density class in which fraction enriched after the separation process
ICP-MS [%]	Element amount from ICP-MS
ICP-MS [mg/kg]	Element mass from ICP-MS
Marked in red	Values from ICP-MS lower than XRF
Marked in green	Elements, which have enriched this fraction in a far higher content to the other density class

EDF upscaling to semi-industrial scale: Exclusion of hercynite

Upscaling electrodynamic fragmentation (EDF) for hercynite samples is impractical, as no comminution was observed in lab-scale tests (D4.1). EDF relies on high-voltage pulses to selectively break materials along grain boundaries or within specific phases. The failure to achieve fragmentation at the lab scale suggests hercynite's properties—such as high hardness, toughness, or uniform composition—make it resistant to the stress waves generated by the process.

Scaling up would increase energy input and equipment size without guaranteeing success, as semi-industrial systems operate on the same principles as lab setups. Inefficiency, energy waste, and higher costs would likely result. Given the lack of comminution at the lab scale, hercynite's fracture behavior is incompatible with EDF, rendering further investment in upscaling unjustifiable.

Limitations of electrodynamic fragmentation for refractory recycling in the ReSoURCE Project

Electrodynamic fragmentation, while a novel and promising technology for certain applications, faces significant limitations when applied to refractory recycling, making it impractical for widespread industrial use in this context. One of the primary issues is its inability to achieve sufficient particle liberation in said materials. Electrodynamic fragmentation relies on high-voltage pulses to create microcracks within the material, ideally separating valuable phases from the gangue. However, refractories are often composed of complex mineral intergrowths with tightly bound phases that do not respond effectively to the stress generated by electrodynamic fragmentation. Instead of achieving clean liberation, the process frequently produces particles that remain partially intergrown, with valuable components still embedded in the matrix. This incomplete liberation severely limits the downstream sorting efficiency, as sensor-based or other dry sorting technologies require high degrees of liberation to differentiate and separate phases effectively.

Additionally, electrodynamic fragmentation is inherently a wet process, requiring the material to be submerged in water to facilitate the propagation of electrical pulses. This poses a significant operational challenge in plants where all other processes are designed as dry systems. Integrating a wet process into an otherwise dry plant introduces complexities such as water management, dewatering, and the handling of slurries, which are not only cost-intensive but also disrupt the streamlined workflow of dry processing facilities. For instance, water recycling systems would need to be installed, increasing capital and operational expenses, and the drying of materials post-fragmentation could lead to energy inefficiencies and logistical bottlenecks. While electrodynamic fragmentation remains theoretically promising for selective material liberation, the technology is not yet advanced enough to deliver economic benefits for refractory recycling. Given the limited time and resources remaining in the ReSoURCE project, this technology will no longer be a focus, allowing efforts to concentrate on approaches with greater immediate applicability and scalability.

3.3 Outcome – Upscaling of comminution methods

This chapter highlights the scalability and limitations of conventional and alternate comminution methods for refractory recycling. Conventional comminution techniques, including jaw, cone, and impact crushers, demonstrated reliable scalability from semi-industrial trials to full-scale industrial applications. The trials showed consistency in particle size distribution, energy efficiency, and wear dynamics, ensuring their direct applicability without the need for further upscaling efforts. These methods remain highly effective and cost-efficient for most refractory recycling scenarios.

In contrast, electrodynamic fragmentation (EDF) faced significant challenges. While promising for specific applications, such as selective liberation of mineral phases, EDF proved ineffective for refractory materials like hercynite, where tightly bound phases resisted fragmentation. Even for MgO-C materials, successful scaling from the selFrag Lab 2.1 to the selFrag PWTS required maintaining precise parameters, highlighting operational complexities. Furthermore, EDF's reliance on a wet process complicates its integration into dry processing plants, introducing additional infrastructure, water treatment, and energy costs.

4. Conclusion

This study underscores the importance of tailored comminution and liberation evaluation methods to optimize the recycling of refractory materials. The complementary use of 2D cross-section analysis and 3D density trials provide a comprehensive framework for understanding material behavior. The 2D approach offers detailed mineralogical insights, capturing fine-scale inclusions and intergrowths that influence liberation. However, its inability to represent the three-dimensional structure of particles limits its scope. Conversely, 3D density trials provide a holistic evaluation of bulk material behavior. Together, these methodologies form a powerful method for analyzing the degree of liberation.

Conventional comminution methods have proven scalable and reliable, with semi-industrial trials demonstrating consistent performance metrics across scales. This confirms their direct applicability to industrial operations without additional upscaling trials, streamlining the transition to full-scale workflows. Their cost-effectiveness and robustness make them the preferred choice for many refractory recycling scenarios.

Electrodynamic fragmentation (EDF), an alternate comminution method, while promising for selectively fragmenting materials along grain boundaries, showed critical limitations when applied to refractory materials. Lab-scale experiments revealed insufficient liberation for tightly bound phases, like in hercynite. Additionally, EDF's reliance on wet processing poses challenges for integration into dry workflows, as it necessitates additional infrastructure for water treatment and drying, which can significantly increase costs. While EDF shows promise for other material types, its current state of development does not align with the specific requirements of refractory recycling.

This research highlights the importance of aligning comminution methods with material properties and operational requirements. A balanced approach, integrating proven methodologies with innovative technologies, offers potential for advancing refractory recycling processes and achieving sustainable, efficient solutions.

5. References

Beckhoff, B., Kanngießer, B., Langhoff, N., Wedell, R., & Wolff, H. (2006). *Handbook of Practical X-Ray Fluorescence Analysis.* Springer.

Thomas, R. (2013). *Practical Guide to ICP-MS: A Tutorial for Beginners.* CRC Press.